*Structural Engineering and Mechanics, Vol. 12, No. 3 (2001) 249-266* 249
DOI: http://dx.doi.org/10.12989/sem.2001.12.3.249

# Investigation of dynamic *P*-Δ effect on ductility factor

Sang Whan Han†, Oh-Sung Kwon‡ and Li-Hyung Lee‡†

*Department of Architectural Engineering, Hanyang University, Seoul 133-791, Korea*

**Abstract.** Current seismic design provisions allow structures to deform into inelastic range during design level earthquakes since the chance to meet such event is quite rare. For this purpose, design base shear is defined in current seismic design provisions as the value of elastic seismic shear force divided by strength reduction factor, $R$ ($\geq 1$). Strength reduction factor generally consists of four different factors, which can account for ductility capacity, overstrength, damping, and redundancy inherent in structures respectively. In this study, $R$ factor is assumed to account for only the ductility rather than overstrength, damping, and redundancy. The $R$ factor considering ductility is called “ductility factor” ($R_\mu$). This study proposes ductility factor with correction factor, $C$, which can account for dynamic ***P*-Δ** effect. Correction factor, $C$ is established as the functional form since it requires computational efforts and time for calculating this factor. From the statistical study using the results of nonlinear dynamic analysis for 40 earthquake ground motions (EQGM) it is shown that the dependence of $C$ factor on structural period is weak, whereas $C$ factor is strongly dependant on the change of ductility ratio and stability coefficient. To propose the functional form of $C$ factor statistical study is carried out using 79,920 nonlinear dynamic analysis results for different combination of parameters and 40 EQGM.

**Key words:** *P*-Δ effect; strength reduction factor; ductility factor.

## 1. Introduction

Current seismic design provisions (UBC 1997, FEMA 1997, SEAOC 1999) allow structures to deform into inelastic range during design level earthquake by adopting strength reduction factor, $R$ which accounts for inherent overstrength and global ductility capacity of structural system. Seismic design provisions define earthquake-induced load using design base shear under design earthquake which is 2/3 of maximum considered earthquake (mean return period of 2475 years). Since the chance of a structure to meet such event is low, it is appropriate to allow structures to deform into inelastic range during such a rare event.

The strength reduction factor, $R$ factor, is introduced in the code formula of design base shear for this purpose. This factor reduces the elastic base shear required to make a structure behave elastically during design level earthquake. The $R$ factor is assigned values not less than 1. Strength reduction factor, $R$, generally consists of four different factors. These four factors account for ductility capacity, overstrength, damping, and redundancy inherent in structures. This study considers only the factor accounting for ductility, which is called as “ductility factor” hereafter.

Since structures are designed using design base shear rather than elastic seismic shear force the

† Assistant Professor
‡ Graduate Student
‡† Professor

structures may experience large story drifts during a large earthquake ground motion such as a design level earthquake ground motion. In this case *P*-Δ effect can be significant, which is defined as the additional deformation induced by a secondary moment. Gravity loads and story drift make this moment.

In the case of an elastic structure with static loading condition story drift including *P*-Δ effect is a little larger than that of first order analysis. When an elastic structure undergoes dynamic loads such as earthquake, the *P*-Δ effect changes natural period of a structure. Thus maximum story drift could increase or decrease depending on the property of the dynamic loads. Also, the earthquake load causes inelastic deformation to a structure since seismic design provisions employ the strength reduction factor, *R* while other design loads such as dead, live, and wind loads do not cause the inelastic behavior to a structure. Thus, the *P*-Δ effect can be significant for seismic design. In current seismic design procedures (FEMA 1997, UBC 1997, SEAOC 1997) the *P*-Δ effect is not well accounted. In those provisions, the *P*-Δ effect is considered by multiplying story drift with numerical coefficient $\alpha$, which is derived from linear static analysis rather than nonlinear dynamic analysis.

Several researchers have carried out studies on the inelastic dynamic *P*-Δ effect of structure. Husid (1969) reported the effect of inelastic dynamic *P*-Δ effect first. Mahin and Boroschek (1992) suggested the methodology to evaluate whether *P*-Δ effect affects bridge structures. MacRae (1994) made recommendations for the design of single degree of freedom structures considering *P*-Δ effect. Recently, Gupta and Krawinkler (2000) carried out two case studies and proposed simple procedure for identifying *P*-Δ effect on MDOF systems.

The purpose of this study is to reflect the dynamic *P*-Δ effect into seismic design procedures. This study attempts to calibrate $R_\mu$ factor using a modification factor, *C* in order to account for dynamic *P*-Δ effect. This factor is considered with the ductility factor in this study since both factors are used for calibrating the base shear, and also they are functions of dynamic properties, response level, and characteristics of earthquake ground motions (EQGMs). In order to establish the functional form statistical study is carried out.

## 2. Strength reduction factor, *R*

Strength reduction factor is adopted in the formula to calculate seismic design base shear. This factor allows a designed structure to deform into inelastic range during a design level earthquake ground motions. The code formula for calculating the design base shear is as follows:

$$V=\frac{C_s}{R}W \tag{1}$$

In Eq. (1) $C_s$ denotes Linear Elastic Design Response Spectrum (LEDRS), *W* is weight of a structure, and *R* is a strength reduction factor. The factor *R* should not be less than 1. In Eq. (1) $C_s/R$ is Inelastic Design Response Spectrum (IDRS). When a building is designed using base shear ($C_s \times W$) without applying *R* factor a structure is expected to behave elastically during a design level earthquake. Fig. 1 shows the conceptual relationship between LEDRS and IDRS. Since *R* is not less than 1 IDRS is less than or equal to LEDRS. In seismic design provisions *R* factor is assigned according to structural systems and structural materials.

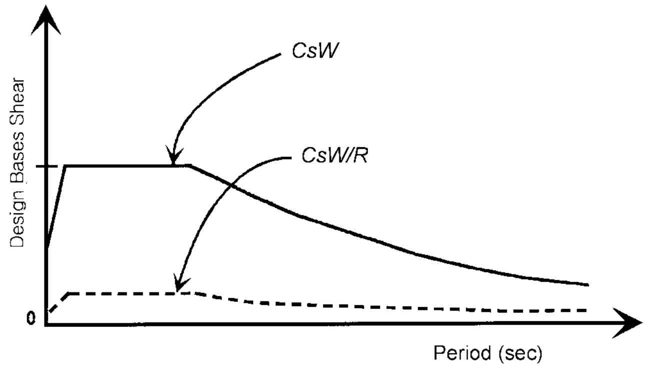


Fig. 1 Design base shear and strength reduction factor

## 3. Ductility factor, $R_\mu$, without consideration of $P$-Δ effect

Strength reduction factor, $R$, generally accounts for ductility capacity, overstrength, damping, and redundancy inherent in structures. Thus $R$ factor can be expressed as follows (ATC 1995):

$$R = R_s \times R_\mu \times R_r \times R_\xi \tag{2}$$

where $R_s$, $R_\mu$, $R_r$, $R_\xi$ are factors which account for overstrength, ductility, redundancy and damping respectively. Many studies have been carried out to evaluate a strength reduction factor, $R$ (ATC 1982, ATC 1995, Bertero 1988).

This study only focuses on ductility factor $R_\mu$. Ductility factor can be defined as the ratio of elastic strength demand ($\mu$=1) to inelastic strength demand for attaining an expected ductility ratio ($\mu$=$\mu_t$) of a structure. Ductility ratio ($\mu$) is the level of inelastic deformation defined as the ratio of absolute value of maximum displacement ($|\mu|_{\max}$) to yielding displacement ($\mu_y$). Ductility factor is defined by following equation:

$$R_\mu = \frac{F_y(\mu=1)}{F_y(\mu=\mu_t)} \tag{3}$$

where $F_y(\mu=1)$ is elastic strength demand and $F_y(\mu=\mu_t)$ is inelastic strength demand for attaining target ductility ratio ($\mu_t$) of a given system.

Ductility factor for a given ductility ratio is evaluated using the procedure shown in Fig. 2. In order to evaluate the strength demand of a single degree of freedom (SDOF) system for a given target ductility ratio and a given earthquake ground motion the following equation of motion is used.

$$m\ddot{u}(t) + c\dot{u}(t) + F(t) = -m\ddot{u}(t) \tag{4}$$

where $m$, $c$, and, $F(t)$ are mass, damping factor, and restoring force, respectively, and $u_g(t)$ is ground displacement. Dot denotes the derivative with respect to time. In this study, the damping ratio is assumed to be 5% of the critical damping for all cases since seismic design provisions are normally based on the 5% damped system. For determining the yield strength, which attains a given target ductility, the iteration process is necessary (Fig. 2).

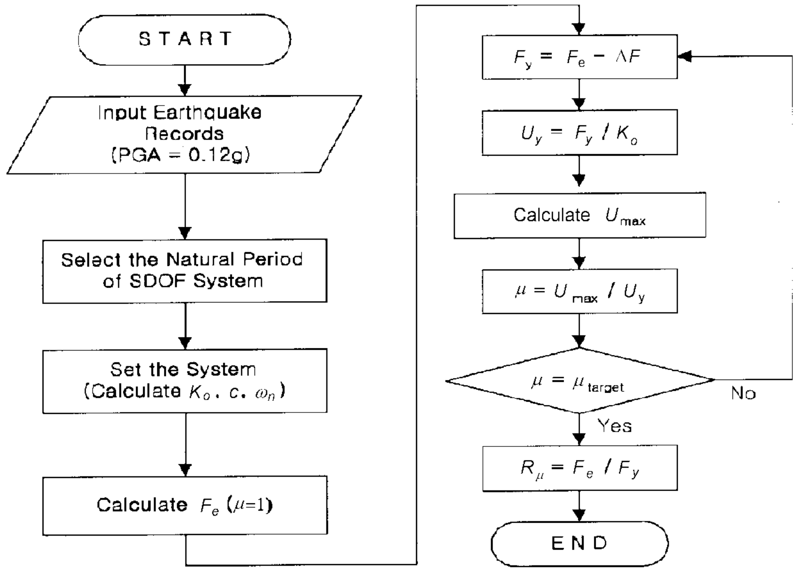


Fig. 2 Procedure for evaluation of ductility factor

## 4. Studies for ductility factor, $R_\mu$

This study adopts the functional form of $R_\mu$ factor proposed by other researchers rather than establishes the functional form for $R_\mu$ factor. Following studies are considered since the functional form of $R_\mu$ factor is adequate to use in this study.

Newmark and Hall (1982) proposed the functional form of ductility factor using elasto-perfectly plastic (EPP) SDOF system as follows.

$$R_\mu = 1.0 \quad \text{for} \quad f \geq 33\text{Hz} (T \leq 0.03 \text{ sec}) \tag{5}$$

$$R_\mu = \sqrt{2\mu - 1} \quad \text{for} \quad 2\text{Hz} \leq f \leq 8\text{Hz} \ (0.12 \text{ sec} \leq T \leq 0.5 \text{ sec}) \tag{6}$$

$$R_\mu = \mu \quad \text{for} \quad f \leq 1\text{Hz} \ (T \geq 1.0 \text{ sec}) \tag{7}$$

Nassar and Krawinkler (1991) evaluated the average IRS of bilinear and stiffness degrading systems subjected to 15 EQGMs recorded on firm soil sites in the Western United States. They proposed a functional form of $R$ factor with respect to ductility ratio, natural period and second slope of bilinear model. The equation proposed by Krawinkler and Nassar is as follows. Damping coefficient is assumed as 5%.

$$R_\mu = [c(\mu - 1) + 1]^{\frac{1}{c}} \tag{8}$$

where

$$c(T, \alpha) = \frac{T^a}{1 + T^a} + \frac{b}{T} \tag{9}$$

Parameters $a$ and $b$ are obtained by regression analysis, which depend on the 2nd slope of the bilinear model.

Miranda and Bertero (1994) performed a similar study to that of Nassar and Krawinkler (1991).

More earthquake records and soil conditions are considered. They proposed the $R_\mu$–$\mu$–$T$ relationship as follows, which depends on the soil condition (rock, alluvium, soft soil). The followings are proposed function for the $R$ factor

$$R_\mu = \frac{\mu-1}{\phi} + 1 \tag{10}$$

where $\phi = 1 + \frac{1}{10T-\mu T} - \frac{1}{2T}e^{-1.5(\ln(T)-0.6)^2}$ for rock

$\phi = 1 + \frac{1}{12T-\mu T} - \frac{2}{5T}e^{-2(\ln(T)-0.2)^2}$ for alluvium

$\phi = 1 + \frac{T_g}{3T} - \frac{3T_g}{4T}e^{-3(\ln(T/T_g)-0.25)^2}$ for soft soil

where $T_g$ denotes the predominant period of EQGM.

Han *et al*. (1999) also proposed the functional form of $R_\mu$ factor, which accounts for the effect of structural period, target ductility ratio and characteristics of different hysteretic models. In their studies two stage regression analysis was carried out in two dimensional domain for establishing the functional form of $R_\mu$ factor. The functional form of proposed $R_\mu$ factor for each hysteretic model is given in Table 1. $R_\mu$ factor for elasto-perfectly plastic model is as follows:

Table 1 Ductility factors for each hysteretic model (Han *et al.* 1999)

$R_\mu = R(T,\mu)*C_{\alpha 1}*C_{\alpha 2}*C_{\alpha 3}*C_{\alpha 4}$
where $R_\mu$ is ductility factor of elasto-perfectly plastic model. $C_{\alpha 1}, C_{\alpha 2}, C_{\alpha 3}$, and $C_{\alpha 4}$ are modification factors for bilinear model ($\alpha_1$), Strength degradation model ($\alpha_2$), Stiffness degradation model ($\alpha_3$), and Pinching model ($\alpha_4$), respectively.

| Hysteretic model | Variables | Ductility factors |
|---|---|---|
| Elasto perfectly plastic model | $K_0$, $U_y$ | $R_\mu = A_0*(1-\exp(-B_0*T_n))$<br>$A_0 = 0.99*\mu + 0.15$<br>$B_0 = 23.69*\mu^{-0.83}$ |
| Bilinear model | $K_0$, $U_y$, $\alpha_1$ | $C_{\alpha 1} = 1.0 + A_1*\alpha_1 + B_1*\alpha_1^2$<br>$A_1 = 2.07*Ln(\mu) - 0.28$<br>$B_1 = -10.55*Ln(\mu) + 5.21$ |
| Strength degradation model | $K_0$, $U_y$, $\alpha_2$ | $C_{\alpha 2} = \frac{1}{A_2*\alpha_2+B_2}$<br>$A_2 = 0.2*\mu + 0.42$<br>$B_2 = 0.005*\mu + 0.98$ |
| Stiffness degradation model | $K_0$, $U_y$, $\alpha_3$ | $C_{\alpha 3} = \frac{(0.85 + B_3*\alpha_3)}{(1+C_3*\alpha_3+0.001*\alpha_3^2)}$<br>$B_3 = 0.03*\mu + 1.02$<br>$C_2 = 0.03*\mu + 0.99$ |
| Pinching model | $K_0$, $U_y$, $\alpha_4$ | $C_{\alpha 4} = \frac{1}{1+0.11*\exp(C_4*\alpha_4)}$<br>$C_4 = 1.4*Ln(\mu) - 0.66$ |

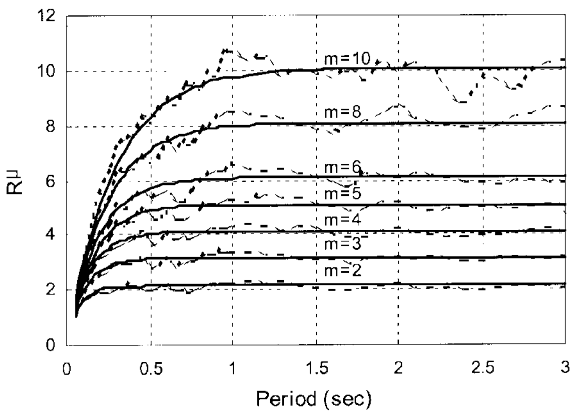


Fig. 3 Fitness of proposed function of $R$ factor by Han *et al.* (1999)

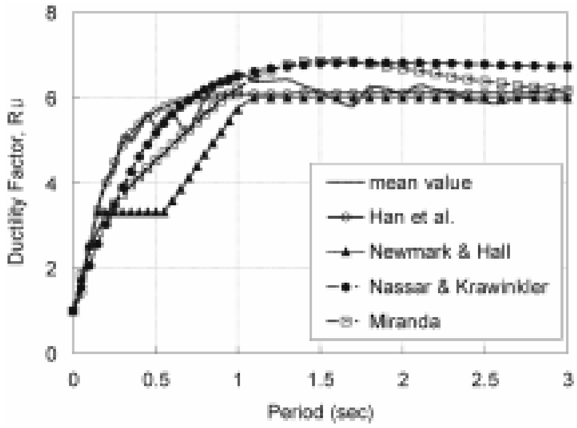


Fig. 4 Comparison of $R_\mu$ factors for soil type 1

$$R_\mu = R(T,\mu) = A_0 \times \{1 - \exp(-B_0 \times T)\} \tag{11}$$

$$A_0 = 0.99 \times \mu + 0.15$$

$$B_0 = 23.69 \times \mu^{-0.83}$$

$R$ factors were computed using 40 earthquake ground motions recorded in soil type 1. Fig. 3 shows the fitness of proposed formula of $R$ factor and actual values which were obtained from nonlinear dynamic analysis using 40 EQGMs. From this figure the fomula of $R_\mu$ factor (Eq. 11) has good precision in the whole range of target ductility ratio and structural periods. Fig. 4 shows the plot for comparison of the values of $R_\mu$ formula proposed by above researchers.

This study adopts the functional form proposed by Han *et al*. (1999) since this proposed formula can account for all different hysteretic effects such as strength and stiffness degradation, and pinching and 2nd slope. Specially these hysteretic effects are significantly correlated with $P$-$\Delta$ effect particularly in inelastic range so that the proposed model (Han *et al.*) is most appropriate with the purpose of this study.

## 5. Code requirement for $P$-$\Delta$ effect

When current seismic design provisions consider $P$-$\Delta$ effect induced by earthquake load seismic force is assumed to be static and the structural period is also assumed to be the same during an earthquake. These can be the weaknesses of current code procedures. In order to account for $P$-$\Delta$ effect the story drift calculated using design base shear is multiplied by $\alpha$ (FEMA 1997) which is defined as follows:

$$\alpha = \frac{1}{1-\theta} \tag{12}$$

where $\theta$ is the stability coefficient which can be calculated by Eq. (13)

$$\theta = \frac{P_x \Delta}{V_x h_{sx} C_d} \tag{13}$$

where $P_x$ = total vertical design load at and above Level $x$
$\Delta$ = design story drift occurring simultaneously with $V_x$.
$V_x$ = the seismic shear force acting between Level $x$ and $x$–1
$h_{sx}$ = story height below Level $x$
$C_d$ = deflection amplification factor.

Design story drift, $\Delta$ shall be computed as the difference of the deflections ($C_d$ times the deflection from elastic analysis using $V_x$). In the provisions, the stability coefficient, $\theta$, shall not exceed following value:

$$\theta_{\max} = \frac{0.5}{\beta C_d} \leq 0.25 \tag{14}$$

where $\beta$ is the ratio of shear demand to shear capacity for the story.

However, Eq. (12) is derived from linear elastic structure under static loading condition as mentioned earlier. However, earthquake excitation is dynamic load and a structure can experience inelastic deformation during an earthquake. Also, structural period can be changed. In this case the $\alpha$ needs to be modified.

## 6. Model for dynamic *P*-Δ effect

A single degree of freedom (SDOF) model proposed by Bernal (1987) is used in this study to consider dynamic $P$-$\Delta$ effect. The model is composed of a rigid column, a lumped mass at the top, and a rotational spring at the bottom as shown in Fig. 5(a). Rotational spring is modeled as elasto-perfectly plastic, Fig. 5(b). Thus, after relative displacement reaches yield displacement, the lateral stiffness of the system, not the spring, become negative due to the effect of gravity load, Fig. 5(c). As a result, the resistance function $F$ depends on the relative displacement, $\Delta$, and is affected by the gravity load $P$. From the fact that the sum of moment at a support is zero, one can obtain following equations.

$$K = \frac{K_r}{H^2} - \frac{P}{H} = K_0(1-\theta) \tag{15}$$

where $K$ is the lateral stiffness, $K_0$ is the value when $P$=0, $H$ is the height, and $\theta$ is the stability coefficient. Eq. (15) can be alternatively expressed as follows:

$$F_y = \frac{M_y}{H}(1-\theta) = F_{y0}(1-\theta) \tag{16}$$

where $F_y$ is the yield load, $M_y$ is the yield moment including any gravity and, $F_{y0}$ is equal to $M_y/H$. According to Eqs. (15)-(16) yield load and stiffness is also dependant on the level of stability coefficient. The stability coefficient, $\theta$, characterizes the gravity effect in the load-deformation curve and can be defined as follows.

$$\theta = \frac{P}{K_0 H} \tag{17}$$

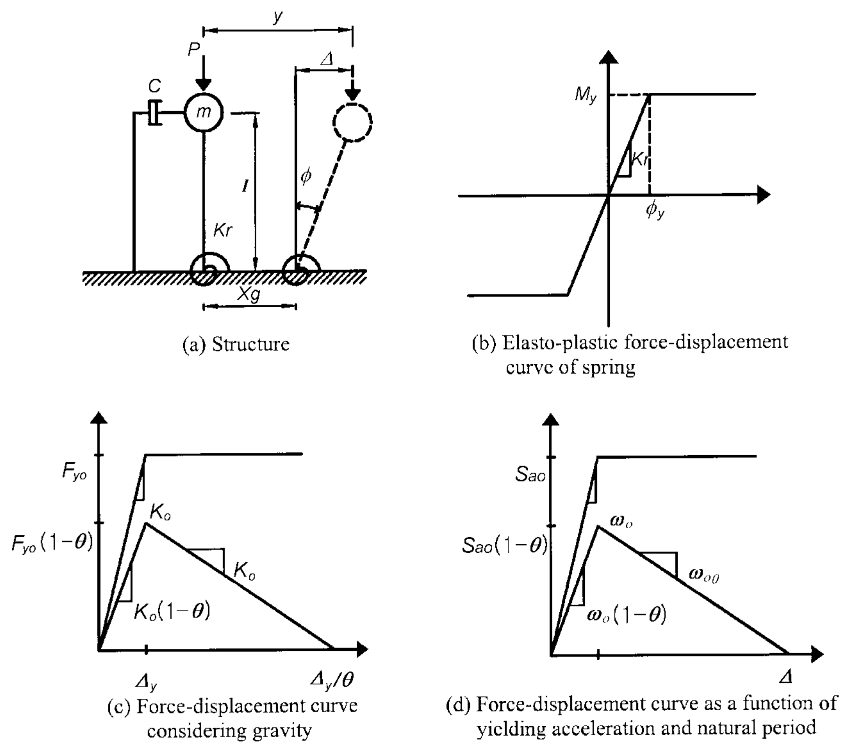


Fig. 5 Structures with considering $P$-Δ effect and without considering $P$-Δ effect

From Eq. (15) and Eq. (17) it can be seen that as the stability coefficient getting larger, the total stiffness of the system becomes smaller. From the fact that the moment about the base must remain at $M_y$ after yielding, one gets

$$\frac{(F-F_y)}{(\Delta-\Delta_y)} = \frac{-P}{H} = -K_0 \cdot \theta \tag{18}$$

With the effect of gravity included in the resistance function, the equation of dynamic equilibrium is shown as follows.

$$\ddot{\Delta}+2\omega_0\xi\dot{\Delta}+\frac{F(\Delta,\theta)}{m} = -\ddot{U}_g(t) \tag{19}$$

where $U_g$ is ground displacement induced by ground excitation, $m$ is mass, $\omega$ is natural cyclic frequency of a system and $\xi$ is damping ratio. The resistance function per unit mass $F(\Delta, \theta)/m$ can also be expressed in terms of the natural frequency of the system shown in Fig. 5(d). Fig. 6 shows the resistance curve as a function of normalized acceleration and maximum displacement. It can be seen from this figure that a structure with consideration of dynamic $P$-Δ effect becomes unstable if maximum ground acceleration is getting larger or the yield strength of its spring is getting lower. Fig. 7 describes the same phenomenon at the view of ductility.

From Fig. 5(c), it is shown that the maximum ductility of static inelastic system, $\mu_s$, is $\theta^{-1}$. While it is theoretically possible for a system to remain stable after a ductility attains or exceeds the static

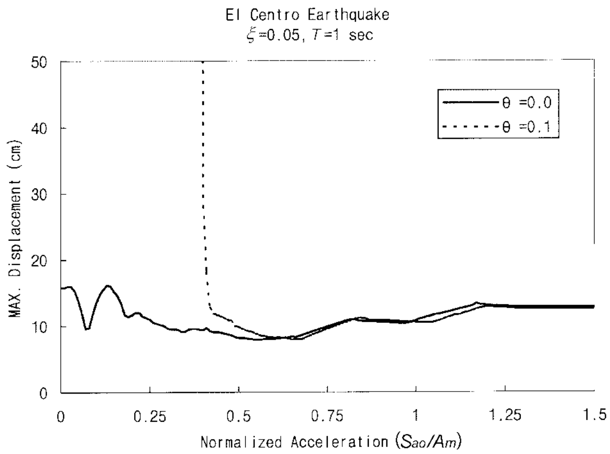


Fig. 6 Effect of stability coefficient on displacement

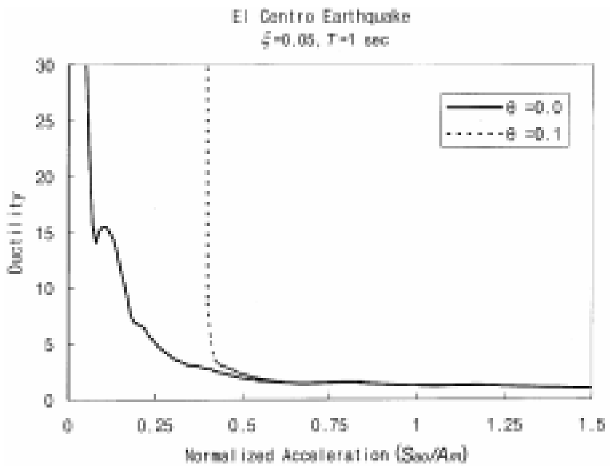


Fig. 7 Effect of stability coefficient on ductility

stability limit, $\mu_s$, extensive numerical results show that the threshold of dynamic instability, $\mu_d$, is much lower than $\mu_s$ for earthquake excitations of significant duration. Bernal (1987) suggested the maximum ductility ratio of inelastic structures under dynamic loading condition as $0.4/\theta$.

## 7. Modification factor considering dynamic *P*-Δ effect

In order to establish the functional form of $R_\mu$ factor, which can account for dynamic *P*-Δ effect, first the ratio between $R_\mu$ factor with ($\theta$ is not 0) and without considering *P*-Δ effect ($\theta=0$) is calculated. This calculation process is repeated for a given set of parameters such as target ductility ($\mu$) ratio, structural period ($T$) and stability coefficient ($\theta$) and for a given earthquake ground motion. Based on obtained $R_\mu$ ratios modification factor ($C$ factor) is regressed with respect to the considered parameters ($\mu$, $T$, $\theta$). The overview of the procedure is shown in Fig. 8 and described in

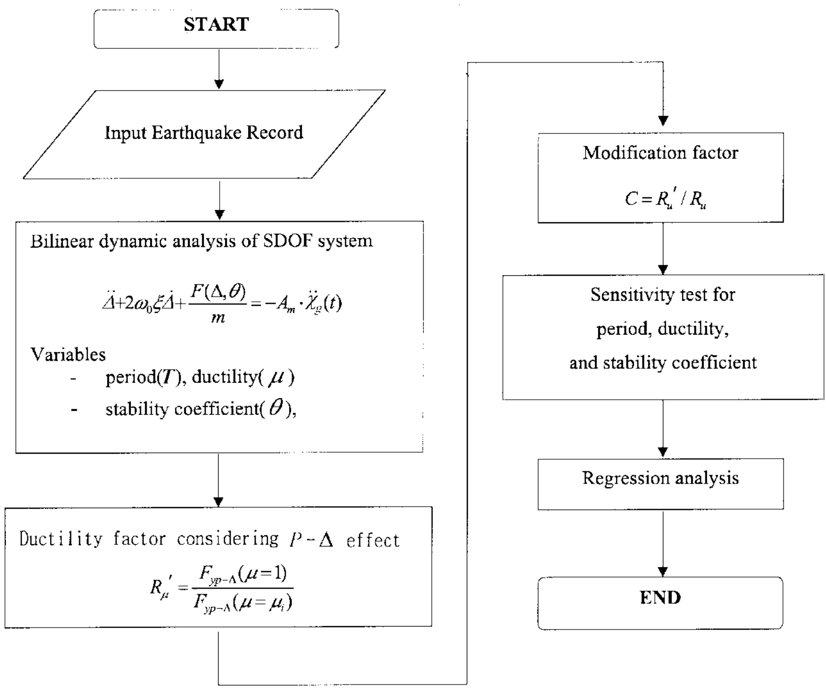


Fig. 8 Procedure for evaluation of modification factor

detail as follows.

### 7.1 Modification factor

Strength factor considering $P$-$\Delta$ effect (hereafter denoted as $R_\mu'$) can be expressed as follows;

$$R_\mu'=\frac{F_{yp-\Delta}(\mu=1)}{F_{yp-\Delta}(\mu=\mu_i)} \tag{20}$$

where $F_{yp-\Delta}(\mu=\mu_i)$ and $F_{yp-\Delta}(\mu=1)$ is inelastic yield strength demand for a given target ductility ratio of $\mu_i$ and elastic strength demand respectively while considering $P$-$\Delta$ effect.

In this study it is assumed that dynamic $P$-$\Delta$ effect is treated as the correction factor of ductility factor as follows:

$$R_\mu'=R_\mu C(\mu,\theta,T) \tag{21}$$

where $R_\mu$ is the strength reduction factor for an EPP model of SDOF system without the effect for gravity. From Eqs. (3), (20) and (21), the following equation is obtained for modification factor $C$.

$$C(\mu,\theta,T)=\frac{F_y(\mu=\mu_i)F_{yp-\Delta}(\mu=1)}{F_{yp-\Delta}(\mu=\mu_i)F_y(\mu=1)} \tag{22}$$

This study assumes that modification factor, $C$, is the function of ductility ratio ($\mu$), structural period ($T$), and stability coefficient ($\theta$).

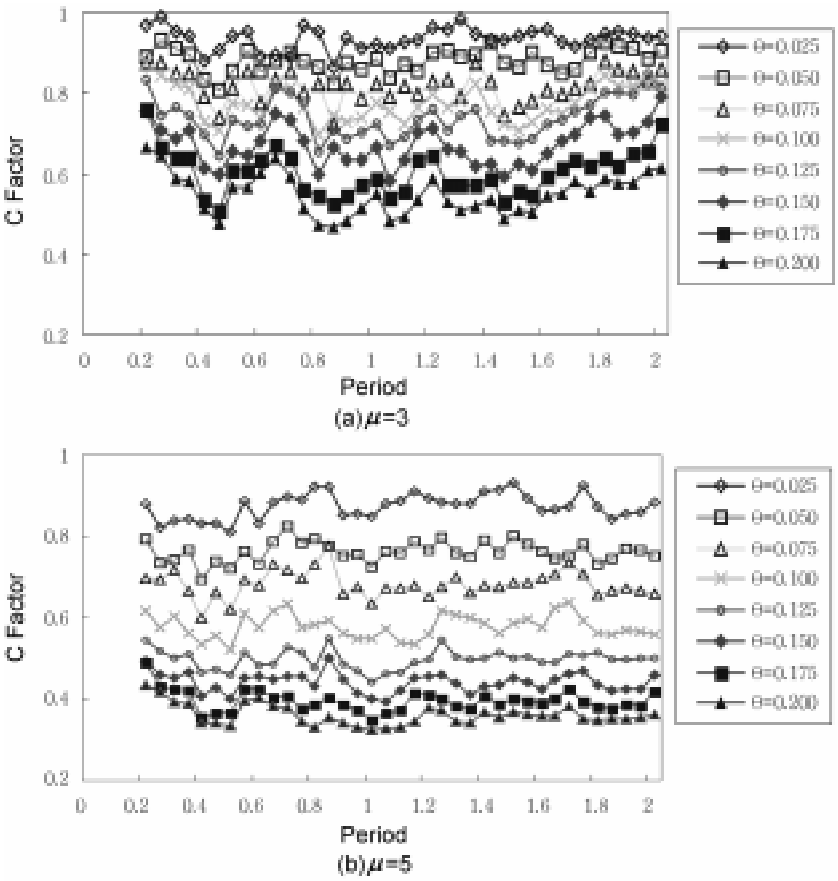


Fig. 9 Relationship between structural period and *C* factor

### *7.2 Sensitivity analysis*

To determine the sensitivity of each parameter on *C* factor the value of *C* is calculated as changing the value of one parameter. During these calculations the other parameters remain constant values. To test the sensitivity following assumptions are made.

1) The modification factor must be 1 for all ductility ratios when stability coefficient is 0.

2) The modification factor must be 0 for all ductility ratios when stability coefficient is 1.

Table 2 shows the inventory of selected EQGMs, which are used in this study. Fig. 9 shows the correlation between structural period and *C* factor. Since the correlation between these two variables is weak with correlation coefficient 0.0341, the effect of structural period on *C* factor is not considered as a parameter for *C* factor.

Table 3 shows the correlation coefficient between structural period and *C* factor for a given target ductility ratio and stability coefficient. Also, the correlations for target ductility ratio vs. *C* factor and stability coefficient vs. *C* factor are tested. Table 4 and Fig. 10 show the correlation coefficient for *C* factor and stability coefficient $\theta$ for a given target ductility ratio of 2. Table 5 and Fig. 11 show the correlation coefficient for *C* factor and target ductility ratio. According to these tables and figures target ductility ratio and stability coefficient strongly affect the *C* factor. As structural period

Table 2 Selected EQGMs

| Earthquake | Station | Date | Magi-nutde (M) | Compo-nent | PGA ($cm/s^2$) | PGV (cm/s) | PGD (cm) |
|---|---|---|---|---|---|---|---|
| Offshore Eureka | Cape Mendocino | 1994.9.1 | 7.2 | 90 | 23.3 | –2.4 | 1.5 |
| Western Washington | Olympia, Washington Hwy Test Lab | 1949.4.13 | 7.1 | 356 | –177.8 | –17.8 | 3.7 |
| Western Washington | Olympia, Washington Hwy Test Lab | 1949.4.13 | 7.0 | 86 | 274.6 | 17.0 | * |
| Whittier | Pacoima-Kagel Canyon | 1987.10.1 | 6.1 | 90 | 154.9 | 7.7 | 1.0 |
| Iwate Prefecture | Miyako Harbor Works, Ground | 1970.4.1 | 5.8 | NS | –189.7 | –4.4 | –0.3 |
| Iwate Prefecture | Miyako Harbor Works, Ground | 1970.4.1 | 5.8 | EW | 161.8 | 3.3 | –0.3 |
| Michoacan, Mexico | Calete De Campo | 1985.9.19 | 8.1 | N90E | 137.8 | –12.6 | 3.2 |
| San Fernando | Lake Hughes, Array Station 4, CA. | 1971.2.9 | 6.5 | S69E | 168.2 | 5.7 | 1.2 |
| San Fernando | Lake Hughes, Array Station 4, CA. | 1971.2.9 | 6.5 | S21W | –143.5 | –8.6 | 1.7 |
| Humbolt County | Petrolia, California, Cape Mendocino | 1975.6.7 | 5.3 | S60E | –198.7 | 5.9 | 0.6 |
| Humbolt County | Petrolia, California, Cape Mendocino | 1975.6.7 | 5.3 | N30E | 103.0 | –3.3 | 0.4 |
| Kern County | Taft Lincoln School Tunnel | 1952.7.21 | 7.7 | 21 | 152.7 | 15.7 | * |
| Kern County | Taft Lincoln School Tunnel | 1952.7.21 | 7.7 | 111 | 175.9 | 17.7 | * |
| Puget Sound | Olympia, Washington Hwy Test Lab | 1965.4.29 | 6.5 | 176 | 194.3 | 12.7 | * |
| Long Beach | Public Utilities Building | 1933.3.10 | 6.3 | 180 | 192.7 | 29.3 | * |
| Long Beach | Public Utilities Building | 1933.3.10 | 6.3 | 270 | 156.0 | 15.8 | * |
| Imperial Valley | Holtville P.O. | 1979.10.15 | 6.6 | 225 | 246.2 | 44.0 | * |
| Imperial Valley | Calexico Fire Station | 1979.10.15 | 6.6 | 225 | 269.6 | 18.2 | * |
| Coalinga | Parkfield Zone 16 | 1983.5.2 | 6.5 | 0 | 178.7 | 14.7 | * |
| Adak,Alaska,Us | Naval Base | 1971.5.1 | 6.8 | North | 85.38 | –3.22 | 1.40 |
| Alaska Subduction | Cordova, Mt. Eccles School | 1964.7.5 | 5.2 | N196E | 34.20 | 3.48 | 0.51 |
| Alaska Subduction | Chernabura Island | 1983.2.14 | 6.3 | N070E | 46.90 | 3.11 | 0.34 |
| Alaska Subduction | Chernabura Island | 1983.2.14 | 6.3 | N070E | 16.70 | 1.05 | 0.30 |
| Dursunbey | Dursunbey Kandilli Gozlem | 1979.7.18 | 5.2 | NS | 233.77 | * | * |
| Imperial Valley | Cerro Prieto | 1979.10.15 | 6.6 | 135 | 163.20 | * | * |
| Loma Prieta | Anderson Dam, Lest Abutment | 1989.10.18 | 7.1 | 250 | 59.70 | 12.13 | 3.77 |
| Mammoth Lakes | Long Valley Dam Left Abutment | 1980.5.25 | 6.1 | 90 | –75.45 | 7.12 | –3.37 |
| Mammoth Lakes | Long Valley Dam (Right Crest) | 1980.5.25 | 6.1 | 90 | –147.72 | 13.06 | –3.89 |
| Mexicali Valley | Cerro Prieto | 1979.10.10 | 4.1 | S33E | –42.00 | * | * |
| Miyagi Prefecture | Ofunato Harbor, Jetty | 1978.6.12 | 6.3 | E41S | –222.1 | 14.10 | –5.10 |
| Miyagi Prefecture | Ofunato Harbor, Jetty | 1978.6.12 | 6.3 | N41E | –206.70 | –12.8 | –2.20 |
| Morgan Hill | Gilroy - Gavilan College | 1984.4.24 | 6.2 | 67 | 94.98 | –3.39 | 0.47 |
| New Ireland | Bato Bridge, Papua New Guinea | 1983.3.18 | 7.7 | 270 | 31.60 | 4.12 | 1.92 |
| San Fernando | 800 W. First Street, 1st Floor, LA | 1971.2.9 | 6.5 | N53W | 138.02 | 19.36 | 9.99 |
| San Salvador | Hotel Sheraton | 1986.10.10 | 5.4 | 0 | 213.90 | –17.67 | –4.55 |
| San Salvador | Hotel Sheraton | 1986.10.10 | 5.4 | 270 | 295.62 | 26.34 | 4.36 |
| Sitka,Alaska | Sitka Observatory | 1972.7.30 | * | North | –70.11 | 10.79 | 9.86 |
| WestMorland | Superstition Mountain, California | 1981.4.26 | 5.6 | 135 | –102.47 | –7.67 | –2.03 |
| Whittier Narrows | Garvey Reservoir-Control Building | 1987.10.1 | 5.9 | 330 | 468.20 | 19.78 | 2.21 |
| Whittier Narrows | LA Griffith Park Observatory | 1987.10.1 | 5.9 | 270 | 133.80 | 7.54 | 0.96 |

NOTE : *denotes unavailable data

Table 3 Correlation coefficient between structural period and *C* factor

| | $\theta$=0.025 | $\theta$=0.050 | $\theta$=0.075 | $\theta$=0.100 | $\theta$=0.125 | $\theta$=0.150 | $\theta$=0.175 | $\theta$=0.200 |
|---|---|---|---|---|---|---|---|---|
| $\mu$=1 | 0.0054 | –0.0738 | –0.0991 | –0.0672 | –0.0334 | –0.0348 | –0.0087 | 0.0631 |
| $\mu$=2 | –0.0220 | –0.0733 | –0.0135 | –0.0044 | –0.0253 | –0.0497 | –0.0076 | –0.0443 |
| $\mu$=3 | 0.1393 | 0.2328 | 0.0253 | 0.0420 | 0.2148 | 0.1356 | 0.0283 | –0.0665 |
| $\mu$=4 | 0.2296 | 0.2221 | 0.0933 | 0.2032 | 0.2230 | 0.0461 | –0.0968 | –0.1810 |
| $\mu$=5 | 0.3404 | 0.1180 | –0.0201 | 0.0290 | 0.0363 | –0.1453 | –0.2455 | –0.3389 |
| $\mu$=6 | 0.5827 | 0.4390 | 0.3781 | 0.2742 | 0.3084 | 0.1127 | –0.0056 | –0.1346 |

Average correlation coefficient: 0.0341

Table 4 Correlation coefficients between *C* factor and stability coefficient $\theta$

| Ductility \ Period | 0.25 sec | 0.50 sec | 0.75 sec | 1.00 sec | 1.25 sec | 1.50 sec | 1.75 sec | 2.00 sec |
|---|---|---|---|---|---|---|---|---|
| 2 | –0.8393 | –0.9821 | –0.9780 | –0.9692 | –0.8586 | –0.8898 | –0.8572 | –0.9611 |
| 3 | –0.9865 | –0.9955 | –0.9727 | –0.9976 | –0.9970 | –0.9917 | –0.9773 | –0.9703 |
| 4 | –0.9842 | –0.9923 | –0.9961 | –0.9904 | –0.9953 | –0.9877 | –0.9980 | –0.9980 |
| 5 | –0.9719 | –0.9782 | –0.9867 | –0.9771 | –0.9883 | –0.9777 | –0.9823 | –0.9785 |
| 6 | –0.9631 | –0.9659 | –0.9737 | –0.9551 | –0.9844 | –0.9623 | –0.9678 | –0.9654 |

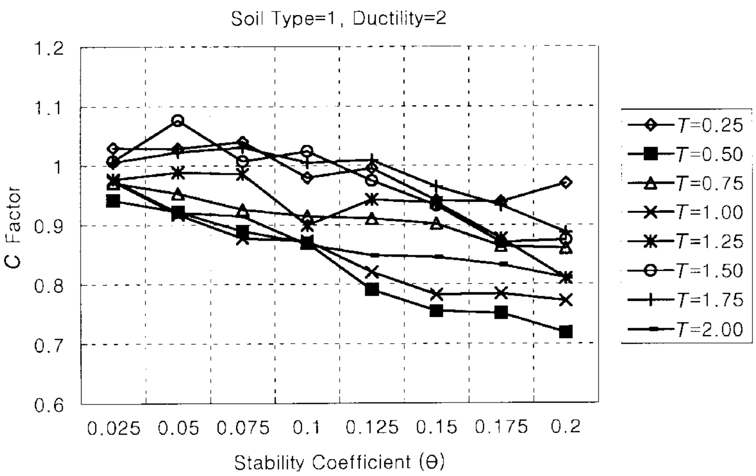


Fig. 10 Correlation between stability coefficient and *C* factor

and *C* factor show little correlation, strength reduction factor for each combination of stability coefficients and ductilities were averaged throughout all periods. Thus Eq. (22) is re-expressed as following equation.

$$C(\mu,\theta,T) \simeq C(\mu,\theta) \tag{23}$$

### 7.3 Functional form of C factor

Regression analysis is carried out to establish the functional form of *C* factor. This analysis adopts

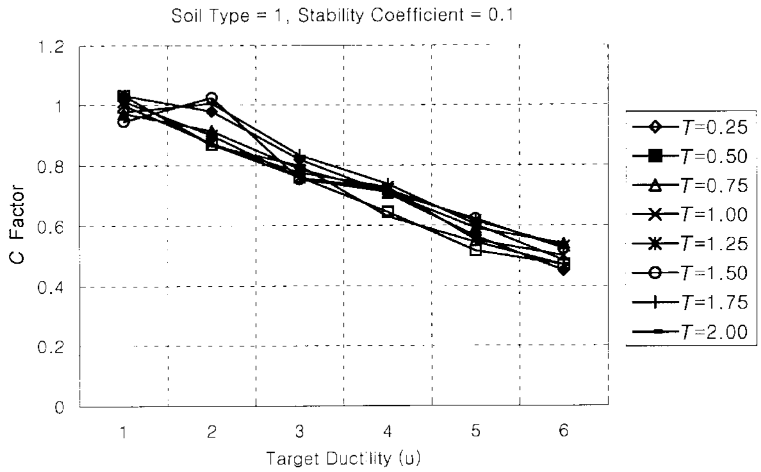


Fig. 11 Correlation between target ductility ratio and *C* factor

Eq. (23) as a basis form of *C* factor. Following combinations of input variables are used. Total 79,920 repetitive calculations of the ratio of $R_\mu$ and $R_\mu'$ (=C) are carried out. Since $R_\mu$ and $R_\mu'$ need to be obtained in each calculation nonlinear dynamic analyses of SDOF system are carried out:

1) Forty earthquake records from rock or stiff soil condition (40)
2) Thirty seven natural periods from 0.2 sec to 2 sec with 0.05 sec interval
3) Nine stability coefficients from 0 to 0.2 with 0.025 interval (9)
4) Six ductility ratios 1, 2, 3, 4, 5, 6 (6)

Table 5 Correlation coefficient between *C* factor and ductility ratio $\mu$

| Stab. Coeff. \ Period | 0.25 | 0.50 | 0.75 | 1.00 | 1.25 | 1.50 | 1.75 | 2.00 |
|---|---|---|---|---|---|---|---|---|
| 0.025 | –0.9419 | –0.9671 | –0.9562 | –0.9267 | –0.9788 | –0.8889 | –0.8480 | –0.8619 |
| 0.050 | –0.9745 | –0.9924 | –0.9961 | –0.9637 | –0.9898 | –0.8718 | –0.9482 | –0.9853 |
| 0.075 | –0.9776 | –0.9905 | –0.9902 | –0.9891 | –0.9772 | –0.9500 | –0.9468 | –0.9846 |
| 0.100 | –0.9949 | –0.9912 | –0.9946 | –0.9903 | –0.9916 | –0.9421 | –0.9760 | –0.9910 |
| 0.125 | –0.9845 | –0.9777 | –0.9881 | –0.9905 | –0.9832 | –0.9676 | –0.9702 | –0.9816 |
| 0.150 | –0.9850 | –0.9624 | –0.9823 | –0.9842 | –0.9728 | –0.9718 | –0.9820 | –0.9766 |
| 0.175 | –0.9769 | –0.9566 | –0.9691 | –0.9759 | –0.9636 | –0.9681 | –0.9757 | –0.9709 |
| 0.200 | –0.9710 | –0.9472 | –0.9600 | –0.9680 | –0.9547 | –0.9573 | –0.9746 | –0.9479 |

Table 6 Modification factor

| $\mu$ | $\theta$=0.025 | $\theta$=0.050 | $\theta$=0.075 | $\theta$=0.100 | $\theta$=0.125 | $\theta$=0.150 | $\theta$=0.175 | $\theta$=0.200 |
|---|---|---|---|---|---|---|---|---|
| 1 | 1 | 1 | 1 | 1 | 1 | 1 | 1 | 1 |
| 2 | 0.9678 | 0.9298 | 0.9021 | 0.8747 | 0.8534 | 0.8349 | 0.8083 | 0.7821 |
| 3 | 0.9060 | 0.8377 | 0.7665 | 0.7230 | 0.6801 | 0.6369 | 0.5697 | 0.5207 |
| 4 | 0.8477 | 0.7481 | 0.6749 | 0.6186 | 0.5563 | 0.5014 | 0.4505 | 0.4091 |
| 5 | 0.8151 | 0.6859 | 0.5994 | 0.5079 | 0.4482 | 0.4000 | 0.3585 | 0.3233 |
| 6 | 0.7880 | 0.6182 | 0.5170 | 0.4248 | 0.3701 | 0.3277 | 0.2926 | 0.2642 |

The results of nonlinear dynamic analyses were fitted to gamma distribution for each ductility and stability coefficients. And the modification factors having exceedance probability of 90% were used in the regression analysis.

Table 6 shows the values of the $C$ factor. This factor becomes smaller as either $\theta$ or $\mu$ is larger. The shaded area contains the values that do not meet the ductility limitation ($u_m = 0.4/\theta$, Bernal).

The function of modification factor from the regression analysis is obtained as follows.

$$C(\mu,\theta)=(1-(1.5911\mu-2.8749)\theta)\cdot(1-\theta) \tag{24}$$

where $$\mu \le \frac{0.4}{\theta}$$

Fig. 12 shows the fitness of the values obtained from regression equation and actual values. From this figure, the function of $C$ factor represents the actual values of $C$ factor with good precision. Fig. 13 shows the overall effect of strength reduction factor, $R_\mu'$ ($T = 2.5$ sec), with consideration of dynamic $P$-$\Delta$ effect. The figure shows that the larger the stability coefficient, the smaller the

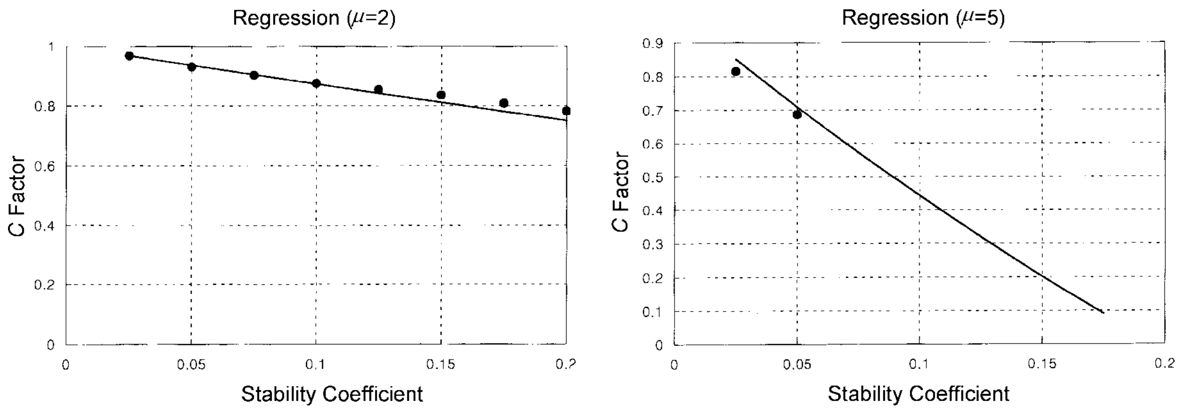


Fig. 12 Fitness of calculated value vs. actual values ($\mu$=2, 5). ( ● Correction Factor, – Regressed Line)

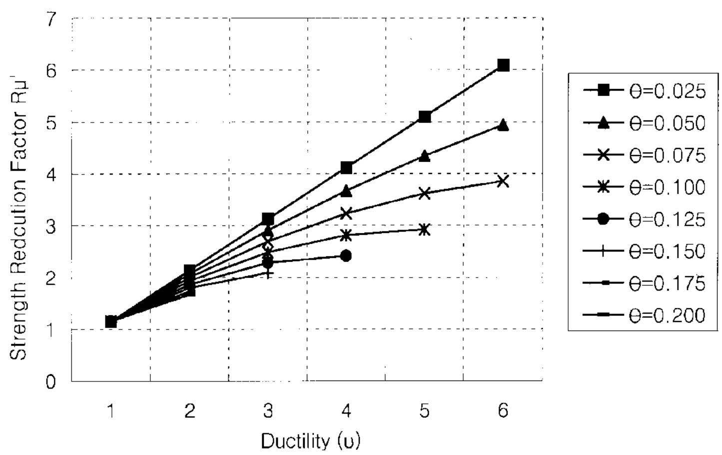


Fig. 13 Effect of the dynamic $P$-$\Delta$ effect ($T$=2.5 sec)

strength reduction factor.

## 8. Validity of proposed $R_\mu'$ function

To verify the validity of proposed $R_\mu'$ factor in Eqs. (11), (21) and (24) 10 earthquake acceleration records from soil type 1 are selected as shown in Table 6 which are different set of records from that shown in Table 2. As the procedure described above, nonlinear dynamic analyses are performed and ductility factors were calculated regarding periods, stability coefficients, and ductility for each earthquake ground motion in Table 7. Fig. 14 and Fig. 15 show the actual (from nonlinear dynamic analysis) and calculated $C$ factor (from proposed formula) with respect to stability coefficient for two different set of structural period and target ductility ratio. From these figures the proposed

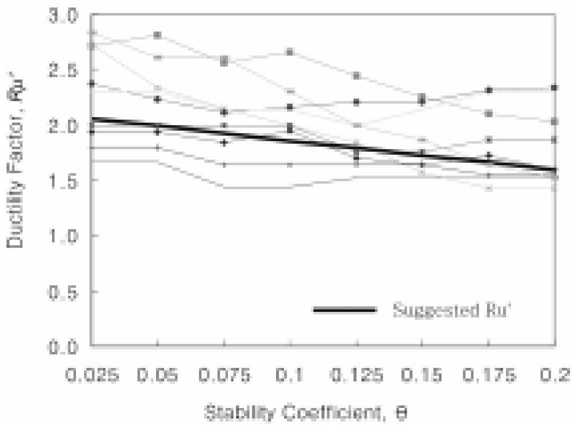


Fig. 14 Ductility factor considering $P$-$\Delta$ effect ($T$=2 sec, $\mu$=2)

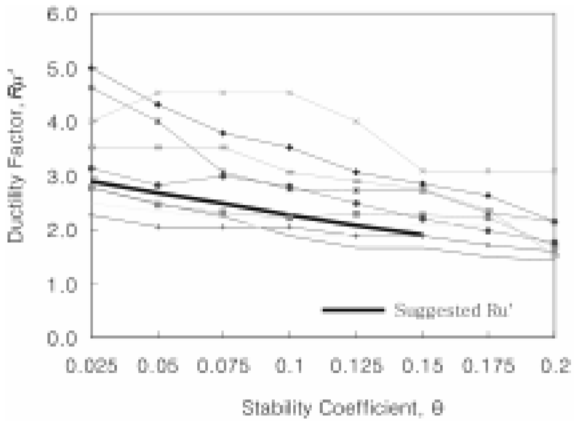


Fig. 15 Ductility factor considering $P$-$\Delta$ effect ($T$=1 sec, $\mu$=3)

Table 7 Selected EQGMs to validate suggested $R_\mu'$

| Earthquake | Station | Date | Maginutde (M) | Compo-nent | PGA (cm/s$^2$) | PGV (cm/s) | PGD (cm) |
|---|---|---|---|---|---|---|---|
| Alaska Subduction | Chernabura Island | 1983.2.14 | 6.0 | N070E | 16.7 | 1.0 | 0.3 |
| Imperial Valley Main Shock | Cerro Prieto | 1979.10.15 | 6.6 | S33E | 163.1 | 13.0 | 3.2 |
| West Morland | Superstition Mountain, California | 1981.4.26 | 5.6 | 135 | 102.5 | 7.6 | 2.0 |
| Miyagi Prefecture | Ofunato Harbor, Jetty | 1978.6.1 | 6.3 | E41S | −222.1 | 14.1 | −5.1 |
| Taft | Taft Lincoln School Tunnel | 1952.7.21 | 7.7 | S69E | −175.9 | 17.64 | 10.14 |
| Mammoth Lakes | Long Valley Dam (Central Recorder) | 1980.5.25 | 6.4 | 90 | −134.6 | 9.4 | −2.7 |
| Michoacan | Calete De Campo | 1985.8.25 | 8.1 | N90W | 81.4 | 6.36 | −1.60 |
| New Ireland | Bato Bridge, Papua New Guinea | 1983.3.18 | 2.5 | 270 | −31.6 | 4.08 | 1.92 |
| Michoacan, Mexico City | La Union | 1985.9.19 | 8.1 | N90E | −147.0 | 11.7 | 4.1 |
| Whittier | Pacoima–Kagel Canyon | 1987.10.1 | 6.1 | 90 | 154.9 | 7.75 | −1.03 |

ductility factor, $R_{\mu}'$ generally agrees in a conservative way with actual values of $R_{\mu}'$ factor.

## 9. Conclusions

The functional form of ductility factor, $R_{\mu}'$ is proposed in this study in order to account for dynamic *P*-Δ effect. Followings are conclusions based on the results of this study.

1) The correction factor $C$ (ratio of $R_{\mu}'$ to $R_{\mu}$) is strongly dependant on the change of ductility ratio and stability coefficient. However, the dependency of this factor on structural period ($T$) is weak.
2) To establish the functional form of $C$ factor the dependency of dynamic *P*-Δ effect on structural period, $T$ is not significant.
3) This study proposed the functional form of $C$ factor with respect to ductility ratio and stability coefficient as follows :

$$C(\mu,\theta)=(1-(1.5911\mu-2.8749)\theta)\cdot(1-\theta)\quad\left(\mu\leq\frac{0.4}{\theta}\right)$$

4) Smaller $C$ factor is obtained as the level of either ductility ratio or stability coefficient increases. This implies that strength reduction factor shall be reduced as the level of either ductility ratio or stability coefficient is increased.
5) Based on the results of this study the $C$ factor varies from 1 to 0.60 according to the level of ductility ratio and stability coefficient. The value 0.60 for $C$ factor represents a strength reduction factor should be 0.6 times smaller than the strength reduction factor obtained without considering the dynamic *P*-Δ effect. Thus, the dynamic *P*-Δ effect gives the significant difference in the results.
6) The proposed equation of $R_{\mu}'$ factor can explicitly account for dynamic *P*-Δ effect for inelastic system.

## Acknowledgements

It is acknowledged that advanced STructural RESearch Station (STRESS) at Hanyang University has supported this study. Also the valuable comments by reviewers are greatly appreciated.

## References

AIK (2000), *Building Design Loads and Commentary,* Architectural Institute of Korea.

ATC-19 (1995), *Structural Response Modification Factors,* Applied Technology Council, Redwood City, California.

ATC-34 (1995), *A Critical Review of Current Approaches to Earthquake-Resistant Design*, Applied Technology Council, Redwood City, California.

Bernal, D. (1987), "Amplification factors for inelastic dynamic P-delta effects in earthquake analysis," *Earthq. Eng. and Struct. Dyn.*, **15**.

Bertero, V.V., Uang, C.M., and Whittaker, A.S. (1988), "Earthquake simulator testing of a concentrically braced steel structure," *Proc. of 9th World Conf. on Earthq. Eng.*, Tokyo-Kyoto, Japan, **8**.

FEMA 302 (1997), *NEHRP Recommended Provisions for Seismic Regulations for New Buildings*, 1997 edn., Federal Emergency Management Agency.

FEMA 303 (1997), *NEHRP Recommended Provisions for Seismic Regulations for New Buildings, Part 2 - Commentary*, 1997 edn., Federal Emergency Management Agency.

Gupta, A., and Krawinkler, H. (2000), "Dynamic P-delta effects for flexible inelastic steel structures," *J. Struct. Eng.*, **126**(1), 145-154.

Han, S.W., OH, Y.H., Lee, and L.H. (1998), "Effect of hystretic model on ductility-based strength reduction factor", *Workshop on Structural Design Issues for Moderate Seismic Zone*, Urbana, Illinois, February.

Husid, R. (1969), "The effect of gravity on the collapse of yielding structures with earthquake excitation," *Proc. of 4th world Conf. on Earthq. Eng.*, Chile, Vol. II, 1969, pages A4-31 to A4-43.

Kilic, S.A., and Krawinkler, H. (1998), "*P*-delta effects in portal frames," *Proc. of the 11th European Conf. on Earthq. Eng.* (Online Version), A. A. Balkema, Rotterdam.

Krawinkler, H. (1995), "New trends in seismic design methodology," *Proc. of 10th European Conf. on Earthq. Eng.*, Duma.

Lee, L.H., Han, S.W., and Oh, Y.H. (1999), "Determination of ductility factor considering different hysteretic models," *J. Earthq. Eng. and Struct. Dyn.*, **28**, 957-977.

MacRae, G.A. (1994), "P-delta effects on single-degree-of-freedom structures in earthquakes." *Earthq. Spect.*, **10**(3), 539-568.

Mahin, S.A., and Boroschek, R.L. (1992), "Influence of geometric nonlinearities on the seismic response of bridge structures," *Proc. of 3rd Workshop on Bridge Engineering Research in Progress*, University of California, San Diego, 211-214.

Miranda (1993), "Site-dependent strength reduction factors," *J. Struct. Eng.*, ASCE, **119**(12).

Miranda, E., and Bertero, V.V. (1994), "Evaluation of strength reduction factors for earthquake resistant design," *Earthq. Spect.*, Earthquake Engineering Research, **10**(2), 357-379.

Nassar, A.A., and Krawinkler (1991), "Seismic demand for SDOF and MDOF systems," John A. Blume EEC, Report No.95, Stanford Univ., CA.

SEAOC (1999), "Recommended lateral force requirements and commentary," Seismology Committee, Structural Engineers Association of California.

UBC (1997), *Structural Engineering Design Provisions*, **2**, *Int. Conf. of Building Officials*.

Vidic, T., Fajfar, P., and Fischinger, M. (1992), "A procedure for determining consistent inelastic design spectra," *Proc. of Workshop on Nonlinear Seismic Analysis*, Slovenia, July.